Chemistry of [1-Cp*-*arachno*-1-IrB_4H_{10}] and [1-Cp*-*arachno*-1-IrB_3H_9]: Synthesis and Characterization of the New Substituted Iridaboranes [1-Cp*-*arachno*-1-IrB_3H_7-2-L], [1-Cp*-*arachno*-1-IrB_2H_6-2-L], and [1-Cp*-*arachno*-1-IrB_4H_8-2,5-$(Br)_2$] (L = PMe_3, PMe_2Ph, $PMePh_2$, py, NEt_3)

Ramón Macías,* Thomas P. Fehlner, and Alicia M. Beatty

Department of Chemistry and Biochemistry, University of Notre Dame, Notre Dame, Indiana 46556-5670

Received January 14, 2004

The treatment of [Cp*IrB_4H_{10}] (**1**) and [Cp*IrB_3H_9] (**2**) with typical Lewis bases afforded the new substituted iridatetra- and iridatriboranes [Cp*IrB_3H_7L] (L = PMe_3 (**3**), PMe_2Ph (**5**), $PMePh_2$ (**7**), PPh_3 (**10**), py (**12**), NEt_3 (**14**)) and [Cp*IrB_2H_6L] (L = PMe_3 (**4**), PMe_2Ph (**6**), $PMePh_2$ (**8**), PPh_3 (**11**), py (**13**), NEt_3 (**15**)), respectively, plus the adduct BH_3L as coproduct. With PPh_3, py, and NEt_3, the formation of the iridapentaborane [1-Cp*-*nido*-1-IrB_4H_8] (**9**) was also observed. The molecular structure of [Cp*IrB_2H_6L] was confirmed by X-ray diffraction analysis on compounds **4**, **8**, and **13**. The substituted iridatetraboranes were found to decompose in solution and in the solid state with decomposition pathways that depend on the nature of the L−B bond and the concentration of the free Lewis bases. Two routes involving the apparent disproportionation of iridaborane−base adducts were found to compete with the loss of a {BH} unit. A reaction cycle driven by the Lewis acid/base chemistry of BH_3 was constructed from these reactions. The P−B bond is labile, leading to ligand exchange with free Lewis bases. For compound **3**, the equilibrium constant for the exchange with PMe_2Ph, $PMePh_2$, and py was measured. In contrast to reaction with nucleophiles, treatment of **1** with bromine and *N*-bromosuccinimide led to the formation of the dibromo- and monobromo derivatives [1-Cp*-1-H-2,5-$(Br)_2$-*arachno*-1-IrB_4H_7] (**16**) and[1-Cp*-1-H-2-Br-*arachno*-1-IrB_4H_8] (**17**), respectively. The molecular structure of **16** was confirmed by X-ray diffraction analysis.

Introduction

Reactions of Lewis bases with polyhedral boron-containing compounds have been investigated ever since the first boron hydrides were prepared.[1,2] In the earlier works, it was found that boranes undergo many reactions with ligands to produce simple Lewis acid−base adducts. Such reactions are known as symmetrical cleavage. Some representative examples are the reaction of B_2H_6 with CO to give BH_3CO[1b] or the formation of $B_3H_7[(CH_3)_3N]$ and $BH_3[(CH_3)_3N]$ from the treatment of B_4H_{10} with trimethylamine.[1c] In contrast, it was also recognized that some Lewis bases promote the unsymmetrical cleavage of boranes to give ionic products. This pathway was observed, for example, in the reactions of diborane(6) with NH_3 and NH_2^-, which afforded $[BH_2(NH_3)_2]^+[BH_4]^-$,[1d,e] and H_2NBH_2 and BH_4^-,[1f,g] respectively. Similarly, the reaction of B_4H_{10} with NH_3 proceeded by unsymmetrical cleavage to yield the salt $[BH_2(NH_3)_2]^+[B_3H_8]^-$.[1h] In some cases, saltlike products were obtained from reactions of Lewis base substituted borane adducts with nonsubstituted boranes. Thus, the reaction of $B_2H_4(PMe_3)_2$ with B_4H_{10} afforded the salt $B_3H_6(PMe_3)_2{}^+B_3H_8{}^-$, which reacts with a slight excess of NMe_3 to give the neutral tetraborane-(8) adduct $B_4H_8(PMe_3)$, in excellent yields.[1i]

Alternatively, polyhedral boranes can react with Lewis bases to form borane adducts with displacement of molecular hydrogen, without cleavage of the cluster framework. Thus, $B_4H_8(CO)$ resulted from the reaction of B_4H_{10} with CO;[2a] similarly, *nido*-decaborane(14), $B_{10}H_{14}$, reacts with CH_3CN to give the bis(adduct) *arachno*-decaborane(12), $B_{10}H_{12}(CH_3CN)_2$, and H_2(g).[2b]

These and other pioneering works on borane adduct chemistry played a role in understanding the cluster-geometry/electron-counting paradigm,[3,4] characteriza-

* To whom correspondence should be addressed. E-mail: rmaza@nd.edu.

(1) (a) Shore, S. G. In *Boron Hydride Chemistry*; Muetterties, E. L., Ed.; Academic Press: New York, 1975; p 79. (b) Burg, A. B.; Schelsinger, H. I. *J. Am. Chem. Soc.* **1937**, *59*, 780. (c) Parry, R. W.; Edwards, L. J. *J. Am. Chem. Soc.* **1959**, *81*, 3554. (d) Schultz, D. R.; Parry, R. W. *J. Am. Chem. Soc.* **1958**, *80*, 4−8. (e) Shore, S. G.; Parry, R. W. *J. Am. Chem. Soc.* **1958**, *80*, 8−12. (f) Schaeffer, G. W.; Basile, L. J. *J. Am. Chem. Soc.* **1955**, *77*, 331. (g) Shore, S. G.; Hickam, C. W., Jr.; Cowles. D. *J. Am. Chem. Soc.* **1965**, *87*, 2755. (h) Hough, W. V.; Edwards, L. J. *Adv. Chem. Ser.* **1961**, *No. 32*, 184. (i) Kameda, M.; Shimoi, M.; Kodama, G. *Inorg. Chem.* **1984**, *23*, 3705.

(2) (a) Brennan, G. L.; Schaeffer, R. *J. Inorg. Nucl. Chem.* **1961**, *20*, 205. (b) Schaeffer, R. *J. Am. Chem. Soc.* **1957**, *79*, 1006.

10.1021/om049960a CCC: $27.50
Publication on Web 03/26/2004

Scheme 1

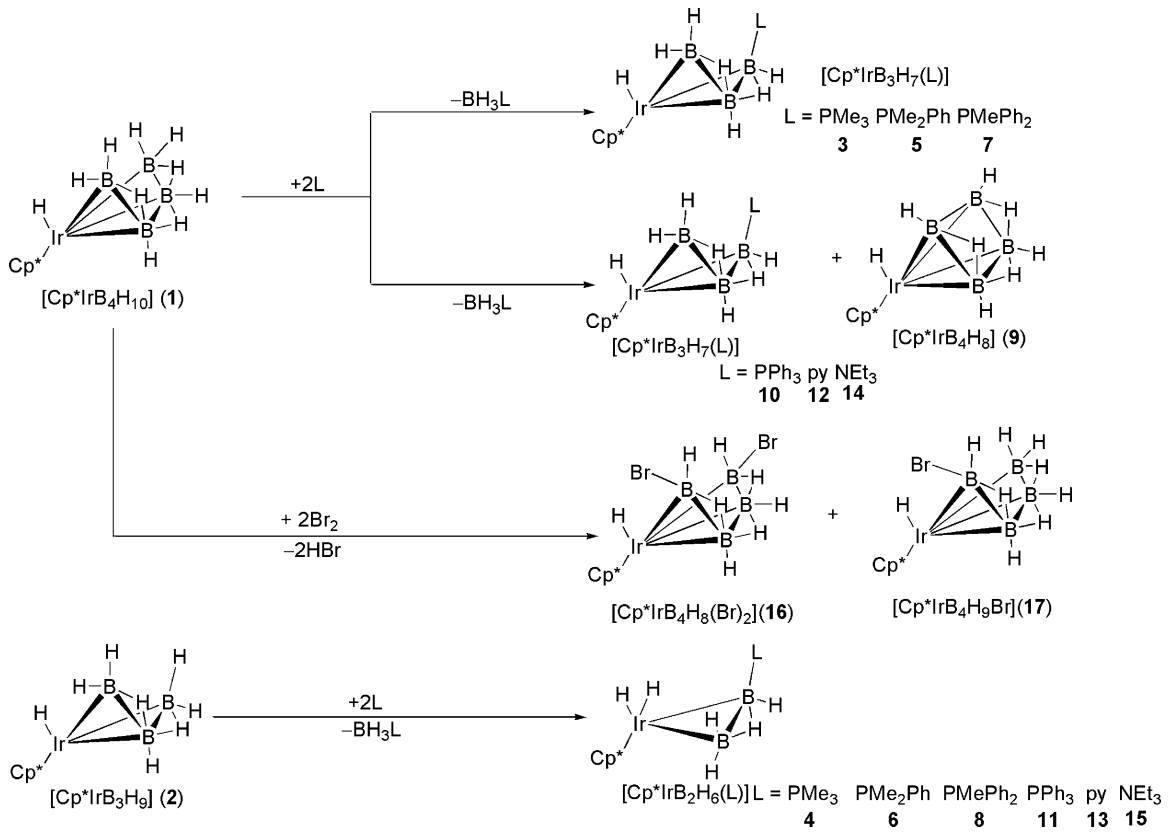

tion of new fluxional processes,[5] and development of synthetic procedures.[1] The preparation of important deltahedral starting materials such as, for example, carboranes utilizes base adduct chemistry.

Reactions of metallaboranes with Lewis bases have been hindered by the lack of good synthetic routes, and systematic studies have been limited to a few cases, including small metal-rich species.[6−8] The development of a general route to metallaboranes via condensation of monoboranes on a metal template now permits a systematic study of their reaction chemistry.[9] Thus, borane displacement by Lewis bases, ligand substitution on boron and metal sites, and ortho metalation of aromatic bases have been reported recently.[10,11] In some aspects, these reactions parallel the early results found with boron hydrides but also illustrate how the presence of transition-metal centers can lead to a different chemistry. Thus, the metal can compete with the boron sites for the Lewis bases, leading, for example, to metal fragment displacement versus borane displacement or ligand substitution at metal sites rather than at a boron site. As transition metals exhibit richer coordination chemistry than p-block elements, they may provide reaction pathways not available to clusters formed exclusively by main-group elements. Therefore, we anticipate that reactions of metallaboranes with Lewis bases will generate new chemistry, involving novel reaction mechanisms, stoichiometric cycles, and the formation of new species with potential applications in synthesis and catalysis. The following describes the chemistry of the five-vertex *arachno*-iridapentaborane [Cp*IrB$_4$H$_{10}$] (**1**) and four-vertex *arachno*-iridatetraborane [Cp*IrB$_3$H$_9$] (**2**) with typical phosphorus and nitrogen bases as well as a typical electrophile.

Results and Discussion

A. Synthesis and Characterization of New Iridaboranes. 1. Structures. [1-Cp*-1-H-*arachno*-1-IrB$_3$H$_6$-2-(L)] and [1-Cp*-1-H-*arachno*-1-IrB$_2$H$_5$-2-(L)]. The reaction of **1** with PMe$_3$, PMe$_2$Ph, PMePh$_2$, PPh$_3$, NC$_5$H$_5$(py), and Et$_3$N causes borane displacement and formation of new phosphine-substituted iridatetraboranes of the general formula [1-Cp*-1-H-*arachno*-1-IrB$_3$H$_6$-2-(L)] (L = PMe$_3$ (**3**), PMe$_2$Ph (**5**), PMePh$_2$ (**7**), PPh$_3$ (**10**), py (**12**), NEt$_3$ (**14**); Scheme 1). These new species are unstable in solution as well as in the solid state, affording the corresponding substituted iridatriboranes of general formula [1-Cp*-1-H-*arachno*-1-IrB$_2$H$_5$-2-(L)] (L = PMe$_3$ (**4**), PMe$_2$Ph (**6**), PMePh$_2$ (**8**), PPh$_3$ (**11**), py (**13**), NEt$_3$ (**15**)).

We were unable to obtain suitable single crystals of [Cp*IrB$_3$H$_7$(L)], but the structures are clear from the spectroscopic data and are in accord with electron-counting rules.[3,4] The molecular ions and fragmentation patterns are in agreement with their formulations. The

(3) Williams, R. E. *Adv. Inorg. Chem. Radiochem.* **1976**, *18*, 67−142.
(4) Wade, K. *Adv. Inorg. Chem. Radiochem.* **1976**, *18*, 1−66.
(5) Gaines, D. F. *Boron Chemistry-4*; Pergamon: Oxford, U.K., 1980.
(6) Housecroft, C. E.; Fehlner, T. P. *Inorg. Chem.* **1986**, *25*, 404−405.
(7) Housecroft, C. E.; Buhl, M. L.; Long, G. J.; Fehlner, T. P. *J. Am. Chem. Soc.* **1987**, *109*, 3323−3329.
(8) Barton, L.; Bould, J.; Fang, H.; Hupp, K.; Rath, N. P.; Gloeckner, C. *J. Am. Chem. Soc.* **1997**, *119*, 631−632.
(9) Fehlner, T. P. *Organometallics* **2000**, *19*, 2643−2651.
(10) Lei, X.; Shang, M.; Fehlner, T. P. *Organometallics* **2000**, *19*, 5266−5272.
(11) Pangan, L. N.; Kawano, Y.; Shimoi, M. *Organometallics* **2000**, *19*, 5575−5581.

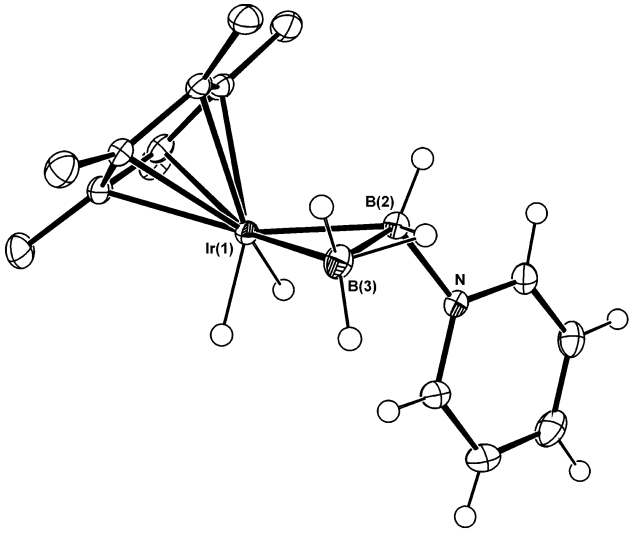

Figure 1. Molecular structure of [Cp*IrB_2H_6(py)] (**13**).

^{11}B NMR spectra of **3** and **5** exhibit a doublet and two triplets in a 1:1:1 ratio; the resonance at the highest field becomes a doublet under proton decoupling, indicating that this is the site of the phosphine substitution. **7** and **10** also exhibit three resonances in the ^{11}B NMR, but the coupling with the hydrogen and the phosphorus atoms were not resolved, due to the broadness of the peaks. The ^{11}B NMR spectra of the phosphine series (**3**, **5**, **7**, **10**) are very similar, whereas those of the nitrogen bases **12** and **14** exhibit the expected shift of the resonance of the N-substituted boron to lower field. The proton NMR spectra show one Cp* signal around 2.00 ppm, four B−H terminal proton resonances between 4 and 2 ppm, two B−H−B bridging hydrogen signals between −1 and −5 ppm, and one Ir−H hydride resonance at high field. In addition, the ^{1}H NMR spectrum of **5** shows two doublets at +1.09 and +0.99 ppm, assigned to the methyl groups of the prochiral phosphine PMe_2Ph. **3** and **7** exhibit only one doublet for the methyl group of the phosphine ligands. The ^{31}P{^{1}H} spectra of **3** and **5** show a broad quartet centered at −9.7 and −5.3 ppm, respectively, whereas the spectra of **7** and **10** consist of a broad peak at 1.1 and 4.8 ppm, respectively. These data are consistent with four-vertex butterfly cluster structures with the iridium atom on a "hinge" position (Scheme 1). The phosphine coordinates a "wingtip" position; therefore, these new compounds are derivatives of **2**[12] in which phosphine substitution results in the loss of a B−H terminal hydrogen atom and one Ir−H hydride: i.e., phosphine-substituted "borallyl" complexes.[13]

Products **4**, **8**, and **13** were characterized by X-ray diffraction analysis (Figure 1, Table 1), and the molecular structures show them to be iridatriboranes consisting of a triangle formed by the organometallic fragment {Cp*IrH_2} and the boron vertices {BH_2} and {BHL} (L = PMe_3 (**4**), $PMePh_2$ (**8**), py (**13**)). Distances and angles given in Table 2 fall within the ranges of existing structural data on related iridaboranes.[12,14,15]

The NMR data of these iridatriboranes are gathered in Tables 3−5 and are fully in accord with the solid-state structures. The ^{11}B{^{1}H} spectra of **4**, **6**, **8**, and **11** exhibit a broad singlet around −18 ppm and a doublet close to −24 ppm, the latter arising from ^1J(B,P) coupling between the substituted boron atom and the phosphorus nucleus of the phosphine ligands. Upon coupling with the proton nuclei, the broad singlet becomes a broad triplet for **4** and **6**, whereas the doublet becomes a doublet of triplets (dt) for **4** and a ddd for **6**. This coupling was not resolved for **8** and **11**, due to the broadness of the peaks. The amine derivatives **13** and **15** show a doublet and a triplet in the ^{11}B NMR spectra, where the doublet corresponds to the N-substituted boron atom and is shifted by about 25 ppm to lower field than the corresponding resonances of the phosphine analogues. The proton NMR shows three B−H terminal resonances and a Cp* signal in the low-field region and B−H−B bridging resonances and Ir−H terminal resonances at high field. The BHB resonances for the phosphine and NEt_3 derivatives appear near −6 ppm, whereas that for pyridine is found at −3.41 ppm. The two Ir−H hydride resonances are found between −16 and −19 ppm.

[^{1}H−^{1}H]-COSY experiments (Tables 3 and 4) and ^{1}H{selective ^{11}B} NMR for **4** and **13** permitted assignment of the resonances. The correlation experiments showed that there are strong cross-peaks between the B−H−B bridging hydrogen and the three terminal B−H hydrogen atoms. This is reflected in the one-dimensional ^{1}H{^{11}B} NMR, in which the resonance of the bridging hydrogen atom is resolved as an apparent quintet for **4** and an apparent quartet for **13**. The two-dimensional spectra also displayed weak cross-peaks between the B−H−B hydrogen atoms and the Ir−H hydrides. Furthermore, the Ir−H hydride atoms exhibited weak cross-peaks with each other and with the Cp* ligands. However, none of these weak off-diagonal signals is manifest in the coupling patterns of the 1D ^{1}H{^{11}B} NMR spectra of **4** and **13**, and the hydride resonances are a singlet and a doublet (^2J(H,P)) for **4** and two singlets for **13**.

[1-Cp*-*nido*-1-IrB_4H_8] (9). The reactions of **1** with PPh_3, pyridine (py), and triethylamine (Et_3N) at room temperature afforded mixtures of the corresponding substituted *arachno*-tetraboranes and *arachno*-iridatriboranes, together with a new species, which was also found to be formed in the conversion of **3** to **4** at high temperature. Of limited stability, this compound could only be characterized spectroscopically in mixtures optimized for its concentration maximum. The data suggest it is the iridapentaborane [1-Cp*-*nido*-IrB_4H_8] (**9**; Scheme 1).

The mass spectrum of the reaction mixture at high concentrations of the iridapentaborane exhibits a broad envelope centered at 376 with a cutoff of *m*/*z* 380 consistent with the parent molecular ion of **9**, $[C_{10}H_{23}B_4Ir]^+$, and some H fragmentation. The ^{11}B{^{1}H} NMR spectrum of **9** shows a singlet at −8.9 ppm that becomes a doublet of triplets in the coupled spectrum. The ^{1}H{^{11}B} NMR spectrum consists of two triplets of

(12) Lei, X.; Shang, M.; Fehlner, T. P. *Chem. Eur. J.* **2000**, *6*, 2653−2664.

(13) Greenwood, N. N.; Kennedy, J. D.; Reed, D. *J. Chem. Soc., Dalton Trans.* **1980**, 196−200.

(14) Boocock, S. K.; Toft, M. A.; Inkrott, K. E.; Hsu, L. Y.; Huffman, J. C.; Folting, K.; Shore, S. G. *Inorg. Chem.* **1984**, *23*, 3084−3091.

(15) Bould, J.; Greenwood, N. N.; Kennedy, J. D.; McDonald, W. S. *J. Chem. Soc., Dalton Trans.* **1985**, 1843−1847.

Table 1. Experimental X-ray Diffraction Parameters and Crystal Data for 4, 8, 13, and 16

	4	**8**	**13**	**16**
empirical formula	$C_{13}H_{30}B_2IrP$	$C_{23}H_{34}B_2IrP$	$C_{15}H_{26}B_2IrN$	$C_{10}H_{23}B_4Br_2Ir$
fw	431.16	555.29	434.19	538.54
cryst dimens (mm)	0.3 × 0.2 × 0.1	0.2 × 0.2 × 0.1	0.2 × 0.2 × 0.1	0.4 × 0.4 × 0.2
space group	$P2_1/c$	$P2_1/c$	$P2_1/n$	$P2_1/n$
a, Å	13.8721(6)	13.3097(7)	13.4635(8)	9.4317(5)
b, Å	8.3612(3)	20.8741(10)	9.4005(6)	13.4815(6)
c, Å	15.1509(6)	8.5511(4)	14.0187(9)	12.5332(6)
α, deg	90	90	90	90
β, deg	101.035(1)	98.543(1)	114.128(1)	99.538(1)
γ, deg	90	90	90	90
V, Å^3	1724.82(12)	2349.4(2)	1619.25(18)	1571.61(13)
Z	4	4	4	4
D(calcd), g cm^{-3}	1.660	1.570	1.781	2.276
μ(Mo Kα), mm^{-1}	7.813	5.756	8.231	13.554
temp, K	100(2)	100(2)	100(2)	100(2)
$2\theta_{max}$, deg	61	56	56	56
transmissn factors	1.00(0.43	1.00(0.73	1.00(0.68	1.00(0.47
no. of rflns collected	20 745	23 451	16 936	16 126
no. of obsd rflns ($I > 2\theta(I)$)	5237	5828	4012	3912
no. of params refined	184	250	198	154
R	0.0216	0.0154	0.0137	0.0252
R_w	0.0534	0.0373	0.0324	0.0638
goodness of fit	1.037	1.085	1.025	1.127
largest peak in final diff map, e Å^{-3}	1.704	1.756	0.828	2.676

Table 2. Selected Interatomic Lengths (Å) and Angles (deg) for [Cp*IrB$_2$H$_6$(PMe$_3$)] (4), [Cp*IrB$_2$H$_6$(PPh$_2$Me)] (8), and [Cp*IrB$_2$H$_6$(C$_5$NH$_5$)] (13)

	4	**8**	**13**
Bond Lengths			
Ir(1)−B(2)	2.146(3)	2.143(2)	2.132(2)
Ir(1)−B(3)	2.157(3)	2.154(2)	2.175(2)
B(2)−B(3)	1.815(4)	1.829(3)	1.828(3)
B(2)−E[a]	1.931(3)	1.930(2)	1.593(3)
Bond Angles			
B(2)−Ir(1)−B(3)	49.89(10)	50.39(8)	50.22(9)
Ir(1)−B(2)−B(3)	65.38(12)	65.11(10)	66.11(10)
Ir(1)−B(3)−B(2)	64.73(12)	64.50(9)	63.68(10)
B(3)−B(2)−E	119.76(18)	118.53(14)	115.05(16)
Ir(1)−B(2)−E	115.22(13)	113.65(10)	119.51(14)

[a] E = P for **4** and **8**, and E = N for **13**.

Table 3. ^{11}B{^{1}H} and ^{1}H{^{11}B} NMR Data for [Cp*IrB$_2$H$_6$(PMe$_3$)] (4) in C$_6$D$_6$ at Room Temperature

assignt[a]	*δ*(^{11}B), ppm	*δ*(^{1}H), ppm[b]	[^{1}H−^{1}H]-COSY
B(2)−H(3)	−24.8[c]	1.59[d]	(3,5)s, (3,4)m, (3,6)s
B(3)−H(4)	−19.1[e]	3.05[f]	(4,5)s, (4,6)s, (4,1)w
B(3)−H(5)		2.83	(5,6)s
μ-H(6)		−6.36[g]	(6,1)w, (6,2)w
Ir(1)−H(1)		−17.06	(1,Cp*)w, (1,2)w
Ir(1)−H(2)		−19.04[h]	(2,Cp*)w

[a] Assignments were made on the basis of ^{1}H{^{11}B(selective)} experiments and [^{1}H−^{1}H]-COSY spectroscopy. [b] Additional ^{1}H NMR data: *δ* 2.13 (s, 15H, Cp*), 0.69 (d, ^2J(HP) = 17 Hz, Me). [c] Site of PMe$_3$ substituent: d, ^1J(BP) = 99; ^{11}B, dt, ^1J(BH) + ^1J(BP) = 113 Hz, ^1J(BH) = 42 Hz. ^{31}P{^{1}H} NMR: d 16.3 (q, ^1J(BP) = 95 Hz, *P*Me$_3$). [d] Broad multiplet, ^nJ(HH) + ^2J(HP) = 10 Hz. [e] Broad triplet, ^1J(BH) = 103 Hz. [f] Broad doublet, ^2J(HH) = 20 Hz. [g] Quintet, ^2J(HH) + ^2J(HP) = 9 Hz. [h] Doublet, ^3J(HP) = 17 Hz.

equal relative intensity at 2.69 and −4.09 ppm, assigned to the B−H terminal and B−H−B bridging hydrogen atoms, respectively, together with a singlet at 2.08 ppm from the Cp* ligand. The relative intensities of the terminal and bridging resonances, calibrated with the known resonances of **10** and **11** present in the reaction mixture, were found to correspond to 4 H each. The proposed structure of **9** is based on a square-planar pyramid with the metal center at the apical position

Table 4. ^{11}B{^{1}H} and ^{1}H{^{11}B} NMR Data for [Cp*IrB$_2$H$_6$(py)] (13) in C$_6$D$_6$ at Room Temperature

assignt[a]	*δ*(^{11}B), ppm	*δ*(^{1}H), ppm[b]	[^{1}H−^{1}H]-COSY
B(2)−H(3)	0.3[c]	3.84[d]	(3,6)s, (3,5)s
B(3)−H(4)	−22.1[e]	3.32	(4,6)s, (4,5)s
B(3)−H(5)		3.20	(5,6)s
μ-H(6)		−3.41[f]	(6,5)s
Ir(1)−H(1)		−16.70	(1,2)w, (1,6)w, (1, Cp*)w
Ir(1)−H(2)		−18.47	(2,1)w, (1,6)w, (2,Cp*)w

[a] Assignments were made on the basis of ^{1}H-{^{11}B(selective)} experiments and [^{1}H−^{1}H]-COSY spectroscopy. [b] Additional ^{1}H NMR data: *δ* 8.45 (d, ^3J(HH) = 6 Hz, 2H, NC$_5$H$_5$), 6.36 (t, ^3J(HH) = 8 Hz, 1H, NC$_5$H$_5$), 5.95 (m, 2H, NC$_5$H$_5$), 2.20 (s, 15H, Cp*). [c] Site of C$_5$NH$_5$ substituent, s; ^{11}B, d ^1J(BH) = 111 Hz. [d] Doublet of doublets, ^2J(HH) 11 Hz, ^3J(HH) 4 Hz. [e] Broad triplet, ^1J(BH) = 103 Hz. [f] Quartet, ^2J(HH) = 10 Hz.

(Scheme 1). Compound **9** is an analogue of the known [1-(CO)$_3$-*nido*-1-FeB$_4$H$_8$] and [1-(Cp)-*nido*-1-CoB$_4$H$_8$].[16,17]

[1-Cp*-1-H-2,5-(Br)$_2$-*arachno*-1-IrB$_4$H$_8$] (16). The reaction of compound **1** with either Br$_2$ or *N*-bromosuccinimide in dichloromethane afforded the dibromo-substituted derivative [1-Cp*-1-H-2,5-(Br)$_2$-*arachno*-1-IrB$_4$H$_7$] (**16**), together with small amounts of the monobromo analogue [1-Cp*-1-H-2-Br-*arachno*-1-IrB$_4$H$_8$] (**17**) (Scheme 1). Both compounds were characterized by spectroscopic means, and the molecular structure was confirmed by X-ray diffraction analysis of **16** (Table 1).

As we were unable to obtain the structure of **1** in our earlier work, that of **16** is worthy of some discussion. The structure is based on an open four-sided pyramidal arachno arrangement, which can be formally obtained by removing two adjacent vertices of connectivity 4 and 5 from a pentagonal-bipyramidal cage (Figure 2). Compound **16** is, therefore, an 8 skeletal electron pair (sep) *arachno*-iridaborane derivative of the parent B$_5$H$_{11}$, with the apical BH group replaced by the isolobal {Cp*Ir} fragment (Figure 2). This structure resembles that found in the isoelectronic group 8 and 9

(16) Greenwood, N. N.; Savory, C. G.; Grimes, R. N.; Sneddon, L. G.; Davison, A.; Wreford, S. S. *J. Chem. Soc., Chem. Commun.* **1974**, 718.
(17) Miller, V. R.; Weiss, R.; Grimes, R. N. *J. Am. Chem. Soc.* **1977**, *99*, 5646−5651.

Table 5. $^{11}B\{^1H\}$ and $^1H\{^{11}B\}$ NMR Data (ppm) for $[Cp^*IrB_2H_6(PMe_2Ph)]$ (6), $[Cp^*IrB_2H_6(PMePh_2)]$ (8), and $[Cp^*IrB_2H_6(PPh_3)]$ (11) in C_6D_6 at Room Temperature[a]

	6[b]		**8**[c]		**11**[d]	
assignt	$\delta(^{11}B)$	$\delta(^1H)$	$\delta(^{11}B)$	$\delta(^1H)$	$\delta(^{11}B)$	$\delta(^1H)$
B(2)−H(3)	−24.3[e]	1.59[f]	−24.9[g]	2.21	−23.1[h]	2.58
B(3)−H(4)	−18.3	3.06[i]	−18.3	3.18	−16.7	3.21
B(3)−H(5)		2.83		3.03		3.09
μ-H(6)		−6.01[j]		−5.71		−5.13
Ir(1)−H(1)		−16.99		−16.96		−17.04
Ir(1)−H(2)		−18.74[k]		−18.50[l]		−17.83[m]

[a] Chemical shifts are given in parts per million. [b] Additional ^1H NMR data: δ 7.48 (m, 1H, Ph), 7.38 (m, 2H, Ph), 7.01 (m, 2H, Ph), 2.11 (s, 15H, Cp*), 1.17 (d, $^2J(HP) = 11$ Hz, 3H, Me), 1.10 (d, $^2J(HP) = 11$ Hz, 3H, Me). [c] Additional ^1H NMR data: δ 7.43 (m, 1H, Ph), 7.03 (m, 1H, Ph), 6.91 (m, 2H, Ph), 2.04 (s, 15H, Cp*), 1.52 (d, $^2J(HP) = 12$ Hz, 3H, Me). [d] Additional ^1H NMR data: δ 7.65 (m, 1H, Ph), 7.63 (m, 2H, Ph), 7.00 (m, 1H, Ph), 2.03 (s, 15H, Cp*). [e] Site of PMe_2Ph substituent: d, $^1J(BP) = 96$ Hz; ^{11}B, br ddd, $^1J(BH) \approx 120$ Hz, $^1J(BP) = 96$ Hz, $^1J(BH) = 42$ Hz. $^{31}P\{^1H\}$ NMR: δ 3.4 (q, $^1J(BP) = 53$ Hz, PMe_2Ph). [f] Broad m, $^nJ(HH) = 9.7$ Hz. [g] Site of $PMePh_2$ substituent: d, $^1J(BP) = 96$ Hz. $^{31}P\{^1H\}$ NMR: δ +10.1 (q, $^1J(BP) = 55$ Hz, $PMePh_2$). [h] Site of PPh_3 substituent: coupling not resolved due to broadness of the peak. $^{31}P\{^1H\}$ NMR: δ +10.0 (br). [i] Doublet, $^2J(HH) = 20$ Hz. [j] Quintet, $^2J(HH) + {}^2J(HP) = 10$ Hz. [k] Doublet, $^3J(HP) = 17$ Hz. [l] Doublet, $^3J(HP) = 17$ Hz. [m] Doublet, $^3J(HP) = 16$ Hz.

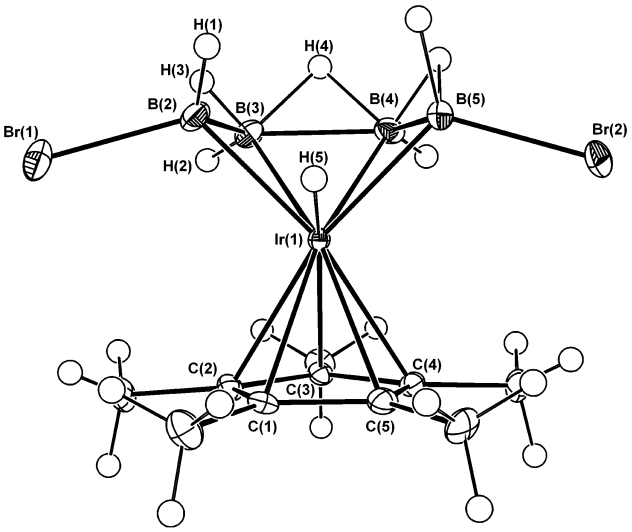

Figure 2. Molecular structure of $[Cp^*IrB_4H_8(Br)_2]$ (**16**).

metallaboranes $[Cp^*FeB_4H_{11}]$,[18] $[(\eta^6\text{-}C_6Me_6)RuB_4H_{10}]$,[19] $[Cp^*CoB_4H_{10}]$,[20] and $[(PMe_2Ph)_2(CO)IrB_4H_9]$.[14]

The NMR data of compound **16** are gathered in Table 6. For comparison, we have also included the spectroscopic data of the parent iridapentaborane **1** and assigned the resonances to the corresponding cluster positions. The ^{11}B NMR spectrum of the bromo derivative exhibits two doublets of equal intensity, and the ^1H NMR spectrum of the boron-bound hydrogen atoms shows a 2:2:2:1:1 relative intensity pattern. In addition, the resonance of the apical Ir−H hydrogen atom appears at the highest field.

The resonances of the bromo-substituted boron atoms in **16** are shifted 7 ppm to low field with respect to **1**. The effect of the bromine atoms is also reflected by a deshielding of the two adjacent BHB bridging hydrogen atoms. In contrast, the unique BHB hydrogen atom and the IrH hydride do not shift significantly upon bromination. The $[^1H\text{-}^1H]$-COSY spectra of **1** and **16** show strong correlations between the two types of bridging hydrogen atoms. The BH terminal hydrogens also exhibit cross-peaks with the BHB bridging hydrogen atoms. The IrH hydride shows weak correlations with terminal and bridging hydrogen atoms of the borane fragment, as well as the methyl groups of the Cp* ring; however, it appears in the ^1H one-dimensional spectrum as a singlet.

2. Properties. Lewis Base Adducts. Compound **1** undergoes facile cleavage with Lewis bases, leading to borane displacement and formation of new boron-coordinated iridatri- and iridatetraboranes. This reactivity pattern reflects preferred substitution at a boron site versus the metal site and stands in contrast with related compounds, e.g. $[(\eta^6\text{-}C_6Me_6)RuB_4H_{10}]$. This *arachno*-ruthenapentaborane also reacts with PMe_3 to give $BH_3{\cdot}PMe_3$, but in the ruthenatetraborane product, $[(\eta^6\text{-}C_6Me_6)(PMe_3)RuB_3H_7]$, the phosphine ligand coordinates to the metal center rather than to the "borallyl" fragment. The nature of the substitution process depends principally on the particular requirements of the metal fragment versus those of the borane fragment.

In the molecular structures of the iridatriboranes [1-Cp*-1-(H)$_2$-*arachno*-1-IrB_2H_4-2-(L)] (L = PMe_3 (**4**), $PMePh_2$ (**5**), NC_5H_5 (**13**)), the substituents at the boron vertices are trans to the Cp* ligand, indicating that steric effects may be important in the final conformation of the molecules. The B−B distance is slightly shorter for the PMe_3 derivative. The average value of the B−B distances of these iridatriboranes, 1.824(4) Å, is longer than the 1.773(8) Å B−B single-bond distance in the ferratriborane analogue, $[(Cp)(CO)_2FeB_2H_5]$,[21] as well as the average distance of the hydrogen-bridged B−B bond (1.744 Å) found in substituted triborane derivatives, $[B_3H_7(L)]$ (L = NCS^-, $NCSe^-$, $NCBH_3^-$, NH_3, CO).[22−25]

The primary mode of M−B bonding in the metallatriboranes appears to be sharing of electron density between the boron−boron bond and a suitable metal orbital, resulting in a MBB three-center−two-electron bond.[21] The average value of the Ir−B distances, 2.151(2) Å, is slightly longer than the sum of the covalent radii (2.08 Å), being consistent with three-center B−Ir−B bonding. On the other hand, the changes of the B−B bond length could be, in part, ascribed to differences in the characteristics of the metal-based vacant orbital (Ir vs Fe). The Ir−B bond distances of the L-substituted boron atoms are somewhat shorter than those of the nonsubstituted boron atoms. This asymmetry suggests that there is a small, but possibly significant, influence of the Lewis bases on the adjacent Ir−B bond. The

(18) Peldo, M. A.; Beatty, A. M.; Fehlner, T. P. *Organometallics* **2003**, *22*, 3698−3702.
(19) Kawano, Y.; Kawakami, H.; Shimoi, M. *Chem. Lett.* **2001**, 1006−1007.
(20) Venable, T. L.; Grimes, R. N. *Inorg. Chem.* **1982**, *21*, 887−895.
(21) Coffy, T. J.; Medford, G.; Plotkin, J. L.; J., G.; Huffman, J. C.; Shore, S. G. *Organometallics* **1989**, *8*, 2404−2409.
(22) Andrews, S. J.; Welch, A. J. *Inorg. Chim. Acta* **1984**, *88*, 153−160.
(23) Andrews, S. J.; Welch, A. J. *Inorg. Chim. Acta* **1985**, *105*, 89−97.
(24) Glore, J. D.; Rathke, J. W.; Schaeffer, R. *Inorg. Chem.* **1973**, *12*, 2175−2178.
(25) Nordman, C. E.; Reimann, C. *J. Am. Chem. Soc.* **1959**, *81*, 3538−3543.

Table 6. ^{11}B and ^{1}H NMR Data (ppm) for [Cp*IrB$_4$H$_{10}$] (1) and [Cp*IrB$_4$H$_8$Br$_2$] (16) in C$_6$D$_6$ at Room Temperature[a]

1				16			
assignt[b]	δ(^{11}B)	δ(^{1}H)[c]	[^{1}H−^{1}H]-COSY	assignt	δ(^{11}B)	δ(^{1}H)[d]	[^{1}H−^{1}H]-COSY
B(2,5)−H(1)	−12.6(2)[e]	+3.47(2)	(1,2)s, (1,3)m, (1,4)s	B(2,5)−H(1)	−5.4(2)[f]	+4.05(2)[g]	(1,2)m, (1,3)s
B(2,5)−H(2)		+2.55(2)[h]	(2,3)s, (2,4)s, (2,6)m				
B(3,4)−H(3)	−4.2(2)[i]	+2.42(2)[j]	(3,4)s, (3,5)s	B(3,4)−H(2)	−7.0(2)[k]	+2.33(2)	(2,3)s, (2,4)s
μ-H(4)		−4.74(2)	(4,5)s, (4,6)m	μ-H(3)		−2.75(2)[l]	(3,4)s, (3,5)w
μ-H(5)		−4.10(1)	(5,1)m	μ-H(4)		−4.16(1)[m]	
Ir(1)−H(6)		−13.82(1)	(6,1)w, (6,Cp*)s	Ir(1)−H(5)		−13.48(1)	(5,1)w, (5,Cp*)m

[a] Chemical shifts are given in parts per million. Relative intensities are given in parentheses. [b] The assignments of the hydrogen atoms H(1) and H(2) are arbitrary; the other assignments were made on the basis of ^{1}H{^{11}B(selective)} experiments and [^{1}H−^{1}H]-COSY spectroscopy. [c] Additional ^{1}H NMR data: δ 1.59 (s, 15H, Cp*). [d] Additional ^{1}H NMR data: δ 1.59 (s, 15H, Cp*). [e] Triplet, ^{1}J(BH) = 130 Hz. [f] Doublet, ^{1}J(BH) = 163 Hz. [g] Doublet, ^{2}J(HH) = 8 Hz. [h] Quartet, ^{2}J(HH) + ^{3}J(HH) = 5 Hz. [i] Doublet of triplets, ^{1}J(BH) = 144, 42 Hz. [j] Quartet, ^{2}J(HH) + ^{3}J(HH) = 4 Hz. [k] Doublet, ^{1}J(BH) = 162 Hz. [l] Quartet, ^{2}J(HH) + ^{3}J(HH) = 8 Hz. [m] Quintet, ^{n}J(HH) = 6 Hz.

Table 7. Selected Interatomic Lengths (Å) and Angles (deg) for [Cp*IrB$_4$H$_8$Br$_2$] (16)

Bond Lengths			
Ir(1)−B(2)	2.178(4)	B(5)−Br(2)	1.998(4)
Ir(1)−B(3)	2.140(4)	B(2)−B(3)	1.845(6)
Ir(1)−B(4)	2.131(4)	B(3)−B(4)	1.838(6)
Ir(1)−B(5)	2.183(4)	B(4)−B(5)	1.841(6)
B(2)−Br(1)	2.004(4)		
Bond Angles			
B(2)−Ir(1)−B(3)	50.57(16)	B(2)−B(3)−Ir(1)	65.78(18)
B(3)−Ir(1)−B(4)	50.97(17)	B(5)−B(4)−Ir(1)	66.20(19)
B(4)−Ir(1)−B(5)	50.52(17)	B(3)−B(4)−Ir(1)	64.79(19)
B(2)−Ir(1)−B(5)	87.14(16)	B(4)−B(3)−Ir(1)	64.25(18)
B(2)−B(3)−B(4)	108.9(3)	Br(2)−B(5)−Ir(1)	119.8(2)
B(3)−B(4)−B(5)	108.1(3)	Br(1)−B(2)−Ir(1)	119.0(2)
B(3)−B(2)−Ir(1)	63.65(18)	B(3)−B(2)−Br(1)	112.8(3)
B(4)−B(5)−Ir(1)	63.28(18)	B(4)−B(5)−Br(2)	114.5(3)

pyridine ligand exhibits the largest difference in the series PMe$_3$, PMePh$_2$, py, as reflected in the degree of shortening of the adjacent iridium−boron bond.

The Intermediate. Compound **9** is analogous to the cobaltaborane [1-Cp*-*nido*-1-CoB$_4$H$_8$]. This species was obtained as the result of the thermal rearrangement of its isomer, [2-Cp*-*nido*-2-CoB$_4$H$_8$], as well as the pyrolytic H$_2$ loss of [1-Cp*-*arachno*-1-CoB$_4$H$_{10}$].[20,26] In contrast, we were unable to isolate **9** by chromatographic methods. This creates a problem, as it is difficult to account for the difference of stability between the iridapentaborane and its cobalt counterpart. On the other hand, the spectroscopic data strongly support our assignment of **9** as [1-Cp*-*nido*-IrB$_4$H$_8$]. Compound **9** is possibly unstable only under the conditions of the reaction with **1**, i.e., an excess of PPh$_3$, precluding its purification by routine chromatographic techniques.

Bromine Derivatives. The molecular structure of the dibromoiridapentaborane **16** indicates C_s symmetry with the mirror plane passing through the iridium atom, the hydride ligand, and the five-membered ring of the η^5-Cp* group. The conformation of the pentamethylcyclopentadienyl ligand is staggered with respect the B$_4$H$_7$Br$_2$ fragment, thereby minimizing the repulsion. The bromine substituents occupy *exo*-polyhedral positions in a cis configuration with respect to the B$_4$ plane of the {B$_4$H$_7$Br$_2$} ligand. The B−Br distances are within the normal ranges found in other metal−boron clusters (Table 7),[27] and the Ir−B and B−B bond lengths compare well with those of the analogous iridapentaborane [(PMe$_2$Ph)$_2$(CO)IrB$_4$H$_9$].[14] This crystal structure contrasts with the C_1 symmetry found for the isoelectronic ruthenaborane [(η^6-C$_6$Me$_6$)RuB$_4$H$_{10}$],[19] in which the unique apical H atom bridges a Ru−B edge.

Both the ^{11}B and the ^{1}H NMR spectra of **16** agree with the C_s symmetry found in the solid state. The IrH hydrogen atom does not exhibit coupling with boron atoms, even at low temperatures, demonstrating its metal hydride character. In contrast, the RuH apical hydrogen atom of [(η^6-C$_6$Me$_6$)RuB$_4$H$_{10}$] displays strong coupling with the boron atoms, B(2) and B(5), indicating its RuHB bridging character and fluxional behavior in solution. These results suggest that the iridium center has a higher tendency than the ruthenium fragment to retain the unique apical hydrogen atom. This affinity is also observed in *arachno*-[(Cp*Ir)$_2$B$_2$H$_8$], in that it does not decompose to give *nido*-[(Cp*Ir)$_2$B$_2$H$_6$], even though both *nido*-[(Cp*M)$_2$B$_2$H$_6$] species (M = Co, Rh) exist.[12,20,28,29] Possibly the strong Ir−H bond ultimately determines the substitution of Lewis bases to the boron, whereas the Ru−H−B bond favors the substitution at the metal site.

B. Reactions and Mechanisms. 1. Characteristics of the Reactions. Reactions of 1 with Lewis Bases. The reactions of the five-vertex *arachno*-iridapentaborane **1** with PMe$_3$, PMe$_2$Ph, and PMePh$_2$ (eq 1, Scheme 1) was complete in a few minutes and quantitatively gave the four-vertex iridatriboranes and the borane adduct. In contrast, **1** reacted more slowly with

$$[Cp^*IrB_4H_{10}] + 2L \rightarrow [Cp^*IrB_3H_7(L)] + BH_3{\cdot}L \quad (1)$$

PPh$_3$, py, and NEt$_3$ with relative rates in the order PMe$_3$ ≈ PMe$_2$Ph ≈ PMePh$_2$ > py > PPh$_3$ > NEt$_3$ for comparable concentrations.

For the reaction of **1** with PPh$_3$ changes in the concentrations of the reactants and products versus time are shown in Figure 3 with an initial **1** to PPh$_3$ ratio of 1:5. The initial slope of the plot of **10** is nonzero, whereas those for **9** and **11** appear to be zero. Hence, the data exhibit the classic time behavior for a consecutive series of reactions where **10** is intermediate in the formation of **9** and **11**. In contrast to **11**, **9** slowly decomposes. When the ratio **1**:PPh$_3$ is reduced to 1:2 (at approximately the same absolute concentration of **1**), the same qualitative profile is observed (Figure 4). However, the

(26) Nishihara, Y.; Deck, K. J.; Shang, M.; Fehlner, T. P.; Haggerty, B. S.; Rheingold, A. L. *Organometallics* **1994**, *13*, 4510−4522.
(27) Stockman, K. E.; Boring, E. A.; Sabat, M.; Finn, M. G.; Grimes, R. N. *Organometallics* **2000**, *19*, 2200−2207.
(28) Lei, X.; Shang, M.; Fehlner, T. P. *J. Am. Chem. Soc.* **1999**, *121*, 1275.
(29) Lei, X.; Bandyopadhyay, A. K.; Sabat, M.; Fehlner, T. P. *Organometallics* **1999**, *18*, 2294.

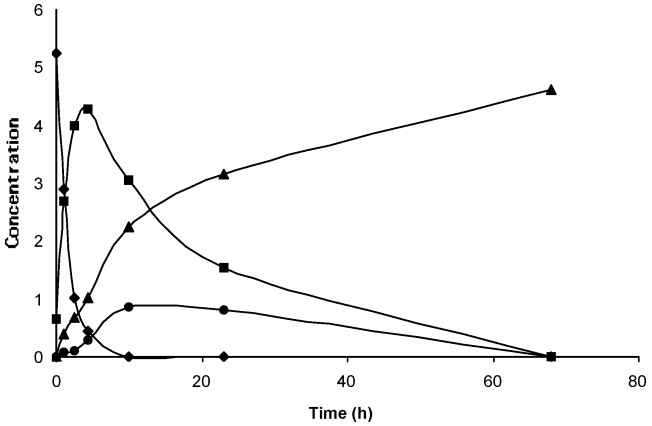

Figure 3. Relative concentration change of reactants and products in the reaction of **1** with 5-fold excess of PPh_3: (◆) **1**; (●) **9**; (■) **10**; (▲) **11**.

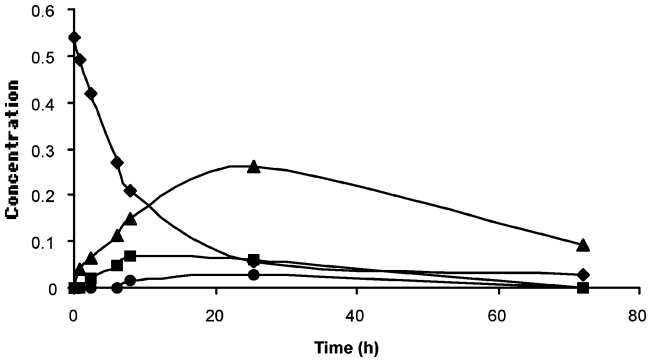

Figure 4. Plot of concentration vs time for the reaction of **1** with PPh_3 in a 1:2 ratio: (◆) **1**; (●) **9**; (■) **10**; (▲) **11**.

decay of **1** is much slower and the maximum in **10** is much lower. Both are consistent with **1** being consumed in a process that depends strongly on phosphine concentration, whereas the loss of the initial product **10** is converted into **9** and **11** in a process that does not depend strongly on phosphine concentration.

Reactions of 2 with Lewis Bases. The reactivity of [1-Cp*-1-H-*arachno*-1-IrB_3H_8] (**2**) with the same Lewis bases (Scheme 1) was examined. The reactions of **2** with PMe_3, PMe_2Ph, $PMePh_2$, and py were also completed in minutes, giving quantitatively the corresponding iridatriboranes and the borane adduct (eq 2, Scheme 1).

$$[Cp^*IrB_3H_9] + 2L \rightarrow [Cp^*IrB_2H_6(L)] + BH_3{\cdot}L \quad (2)$$

Consequently, the substituted iridatriboranes $[Cp^*IrB_2H_6(L)]$ can be prepared directly from **2** via borane displacement and base substitution at a boron site.

In contrast, with PPh_3 the reaction was completed in 4 h, whereas with NEt_3 we observed reaction completion after 16 h. The relative rates follow the trend $PMe_3 \approx PMe_2Ph \approx PMePh_2 \approx$ py > PPh_3 > NEt_3. PPh_3 and py react faster with compound **2** than with compound **1**.

Conversion of 3 to 4. The substituted iridatetraboranes **3**, **5**, **7**, **10**, **12**, and **14** are unstable in solution as well as in the solid state, affording the corresponding substituted iridatriboranes (eq 3, Scheme 2). This

$$[Cp^*IrB_3H_7(L)] \rightarrow [Cp^*IrB_2H_6(L)] + \{BH\} \quad (3)$$

conversion involves formally a {BH} loss, which has

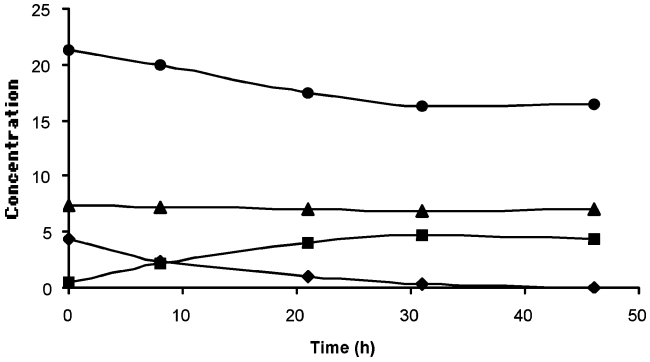

Figure 5. Relative concentration changes for the transformation of **3** (◆) to **4** (■), $BH_3{\cdot}PMe_3$ (▲), and total boron concentration (●), after the reaction of 1 equiv of **1** with 2 equiv of PMe_3.

Scheme 2. Reaction Cycle

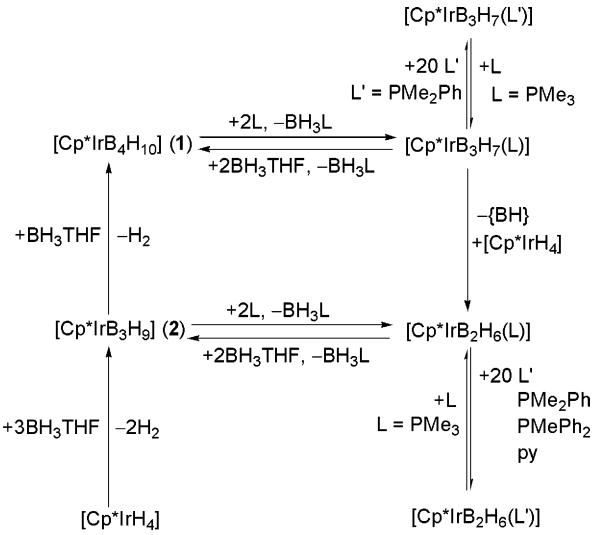

considerable precedent in both borane and metallaborane chemistry.[30,31] However, there is little information in the literature on the chemical fate of the {BH} unit. Therefore, the overall transformation of **3** into **4** was looked at more closely by NMR.

After the reaction of **1** with 2 equiv of PMe_3 to form **3** and BH_3PMe_3 quantitatively, the transformation of **3** into **4** was followed by NMR. Figure 5 shows a plot of the concentrations of **3**, **4**, $BH_3{\cdot}PMe_3$ and total boron against time. In about 9 h the initial concentration of **3** decreased by half and an equivalent concentration of **4** is produced. In nearly 30 h, **3** has been converted quantitatively to **4**. The total boron loss corresponds to the initial concentration of **3**; therefore, a {BH} fragment is "literally" lost in the process. Close examination of the NMR tube showed formation of a white precipitate that was insoluble in C_6D_6, CH_2Cl_2, and THF.

In contrast, the same study for a 1:7 ratio of **1** to PMe_3 gave the results plotted in Figure 6. Note the time scale is now days, not hours. After 40 days the conversion still did not reach completion, showing that excess phosphine inhibits the conversion of **3** to **4**. In addition, there was a parallel increase in the concentrations of **4**

(30) Bould, J.; Greenwood, N. N.; Kennedy, J. D. *J. Organomet. Chem.* **1983**, *249*, 11−21.
(31) Morrey, J. R.; Johnson, A. B.; Fu, Y. C.; Hill, G. R. *Adv. Chem. Ser.* **1961**, *No. 32*, 157−67.

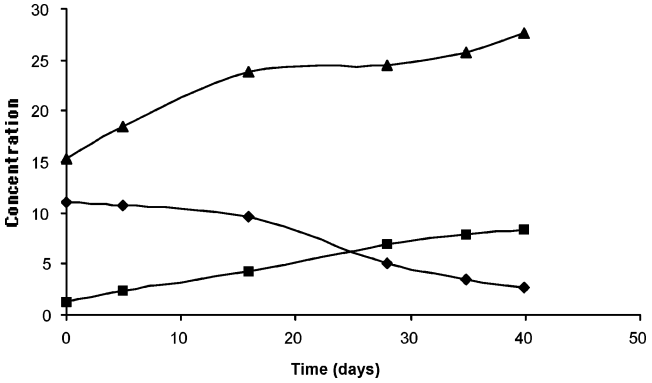

Figure 6. Plot of concentration vs time for the transformation of **3** (◆) to **4** (■) and BH_3·PMe_3 (▲) after the reaction of 1 equiv of **1** with 7 equiv of PMe_3.

Table 8. Summary of Free Reaction Energies (kJ mol^{-1}) and Equilibrium Constants for the Ligand Exchange Reactions of 3 and 4 at 298 K

4 + L′ ⇔ **6**, **8**, **13** + PMe_3 **3** + L′ ⇔ **5** + PMe_3

L′	$\Delta G°$	K_{eq}	$\Delta G°$	K_{eq}
PMe_2Ph	12	8.0×10^{-3}	12	8.0×10^{-3}
$PMePh_2$	23	9.0×10^{-5}		
py	30	6.0×10^{-6}		

and BH_3·PMe_3. The ^{1}H NMR spectra showed formation of [Cp*IrH_4], and the increase in the concentration of the iridium hydride parallels the formation of compound **4**, suggesting that both species are formed simultaneously. Not only does phosphine inhibit the conversion of **3** to **4**, but a large excess permits a second, less efficient reaction channel to be utilized. Thus, ligand exchange properties of **3** were examined.

Ligand Exchange Reactions. The iridatetraborane **3** undergoes a ligand exchange reaction with PMe_2Ph (eq 4, Scheme 2).

$$[Cp^*Ir_3H_7(PMe_3)] + PMe_2Ph \leftrightarrow [Cp^*Ir_3H_7(PMe_2Ph)] + PMe_3 \quad (4)$$

Similarly, we found that iridatriborane **4** undergoes exchange of PMe_3 with an excess of PMe_2Ph at low temperatures. At high temperature, the exchange of PMe_3 in compound **4** with an excess of PMe_2Ph and py is accompanied by decomposition of the iridatriborane with formation of [Cp*IrH_4] and BH_3·L. With PPh_3, in contrast, we did not observe either ligand exchange or decomposition of the iridatriborane, even at high temperatures.

The relative intensities of the ^{1}H NMR signals for the L-substituted iridaboranes as a function of temperature allowed the estimation of the equilibrium constants (Table 8). The values of the corresponding free energies reflect the binding energy differences of the Lewis bases. As expected, the more basic PMe_3 ligand forms more stable boron-substituted iridatri- and iridatetraboranes, but the differences are not large and are consistent with facile ligand substitution relative to conversion of **3** to **4**.

Cluster Expansion Reactions. {BH} addition via BH_3·THF is a known method for increasing the size of the borane fragment in metallaboranes, carboranes, and other heteroboranes.[1,32] This is illustrated, for example, in the preparation of **1** from **2**, in which a {BH} unit has been formally added to the iridatetraborane to give the iridapentaborane.[12]

We have found that the treatment of the iridatriboranes **4**, **6**, **8**, **13**, and **15** with BH_3·THF at room temperature gives **2** and BH_3L (eq 5).

$$[Cp^*IrB_2H_6(L)] + 2BH_3 \rightarrow \underset{\mathbf{2}}{[Cp^*IrB_3H_9]} + BH_3{\cdot}L \quad (5)$$

Likewise, the reaction of the iridatetraboranes **3**, **5**, and **7** with BH_3·THF at room temperature afforded **1** and BH_3L (eq 6).

$$[Cp^*IrB_3H_7(L)] + 2BH_3 \rightarrow \underset{\mathbf{1}}{[Cp^*IrB_4H_{10}]} + BH_3{\cdot}L \quad (6)$$

BH_3 cluster expansion and Lewis base displacement regenerates the iridapenta- and iridatetra-boranes, **1** and **2**.

Reaction Cycle. As summarized in Scheme 2, the reactions of **1** and **2** and the new substituted iridaboranes permit a reaction cycle to be constructed. For both the iridapentaborane **1** and iridatetraborane **2**, base displacement of borane and addition of borane to the L-boron-substituted iridaboranes constitute reversible reaction sets. These two reversible reactions are connected by {BH} fragment loss and {BH} fragment addition, thereby generating a four-step reaction cycle. If we consider the whole cycle with species "in" balanced against species "out", the net reaction is

$$3BH_3 + 2L \rightarrow 2BH_3{\cdot}L + \{BH\} + H_2 \quad (7)$$

In the ligand exchange reactions of **4** with PMe_2Ph and py at high temperature, we observed formation of [Cp*IrH_4], which is also formed in the conversion of **3** to **4** in the presence of free phosphine. [Cp*IrH_4] reacts with an excess of BH_3·THF to give compound **1**, presumably through the formation of **2** (Scheme 2).

2. Mechanistic Considerations. The observations described above permit a rudimentary reaction pathway to be described. The reaction rate of **1** with PPh_3 depends on the concentration of the phosphine. A possible first step for this reaction is the formation of an iridapentaborane adduct, [Cp*IrB_4H_{10}(L)], in fast equilibrium with free ligand, L, and compound **1**. In a subsequent rate-determining step, the activated iridaborane adduct reacts with another molecule of L to give BH_3·L and the iridatetraborane [Cp*IrB_3H_7(L)] (Scheme 3).

The substituted iridatetraboranes undergo decomposition through at least two parallel pathways, with contributions to iridatriborane formation that depend on the Lewis base, its concentration, and the conditions of the reaction. Thus, the PPh_3 derivative **10** decomposes, leading to the formation of **9** and **11**. A likely route is the dissociation of the PPh_3−B bond to give a putative 6 skeletal electron pair (sep) species, [Cp*IrB_3H_7], that disproportionates to yield the iridapentaborane **9** and the iridatriborane **11**, both of which are observed as products (Scheme 3, path i).

(32) Kang, S. O.; Sneddon, L. G. *Inorg. Chem.* **1988**, *27*, 3298−3300.

Scheme 3[a]

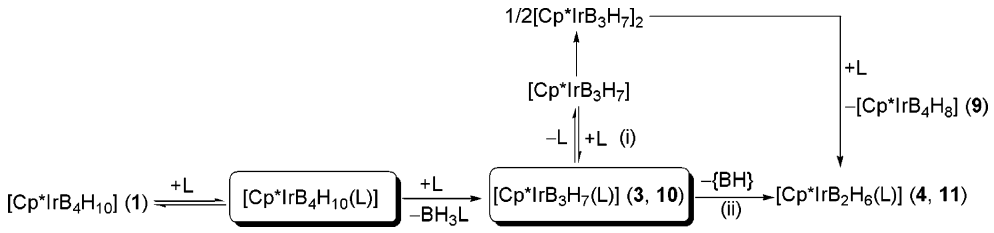

[a] L = PMe_3, PPh_3. Legend: (i) dissociation equilibrium and disproportionation; (ii) {BH} loss via polymer formation.

For PMe_3 decomposition of **3** without free phosphine at room temperature proceeds more rapidly than with PPh_3, and no **9** accompanies the formation of **4**. Loss of {BH} to give an insoluble "polymer" and the substituted iridatriborane **4** (Scheme 3, path ii) is suggested as a parallel path for the formation of the iridatriborane. Since PMe_3 forms stronger P−B bonds than PPh_3, the pathway involving dissociation equilibrium is less favored. This is supported by the measured ligand-exchange equilibrium parameters. However, when the temperature is increased, P−B dissociation becomes more important for PMe_3, and evidence for **9** is found. As the ligand dissociation equilibrium is shifted toward the formation of the intermediate [Cp*IrB_3H_7], path i now contributes to the formation of **9**.

In the reaction of **1** with PPh_3, the yield of **11** is close to 50% when the concentration of **9** is at its maximum value of 15%. These data suggest that at that point at least 30% of **11** arises through the dissociation/disproportionation pathway, whereas almost 70% arises via the polymeric {BH} loss. Thus, in the PPh_3 system both decomposition routes operate simultaneously independently of the conditions, while for PMe_3 at room temperature under stoichiometric conditions the decomposition of **3** follows exclusively the {BH} loss pathway (Scheme 3, path ii).

The mechanism suggested in Scheme 3 is clearly not complete. For example, at room temperature with excess PMe_3, **3** decomposes extremely slowly, giving rise to the simultaneous formation of [Cp*IrH_4], BH_3PMe_3, and **4**. However, the essential aspects of the more facile conversion of **1** to iridatetra- and iridatriboranes are expressed by Scheme 3 and are consistent with our expectations based on known borane and metal cluster chemistry.

Conclusions

The reactivity of a metallaborane is strongly controlled by the metal center. This effect on reactivity is illustrated by the isoelectronic metallapentaboranes [Cp*IrB_4H_{10}] (**1**) and [(η^6-C_6Me_6)RuB_4H_{10}], in which, after BH_3 displacement, the metal centers drive the final attack of the Lewis base, PMe_3, toward the borane fragment and the metal site, respectively.

Metallaborane adducts undergo decomposition following different reaction pathways, depending on the Lewis bases and the conditions of the reaction. The PPh_3 ligand promotes decomposition throughout ligand dissociation and disproportionation, as well as direct {BH} loss. In contrast, an excess of PMe_3 leads directly to disproportionation of the metallaborane adduct and inhibition of {BH} loss. At high temperatures, PMe_3 shares the ligand-dissociation pathway. The nature of the L−B bond determines ultimately the course of the reaction, whereas changes in the conditions vary the relative rates of the different processes, leading to fine-tuning of the reactivity.

We have demonstrated that the reaction of Lewis bases with metallaboranes can generate interesting chemistry which produces new compounds, stoichiometric cycles, and reaction pathways from which insights of fundamental processes such as the decomposition of metallaborane adducts can be gained.

Experimental Section

General Considerations. All reactions were carried out under an argon atmosphere using standard Schlenk-line techniques.[33] Solvents were distilled immediately before use under a dinitrogen atmosphere: sodium benzophenone ketyl for hexanes and tetrahydrofuran and calcium hydride for dichloromethane. All commercial reagents were used as received without further purification. **1** was prepared by the procedure described below, which is a modification of the synthesis reported earlier.[12] NMR spectra were recorded on 400 MHz Bruker and 500 MHz Varian spectrometers. NMR references: internal (C_6D_6, δ_H 7.06 ppm) for ^{1}H; external ([(Me_4N)(B_3H_8)] in acetone-d_6, δ_B −29.7 ppm) for ^{11}B; external (H_3PO_4 in D_2O, δ_P 0.0 ppm) for ^{31}P. All J values are given in Hz. IR spectra were recorded on a Nicolet 205 FT-IR spectrometer; all values are given in cm^{-1}. Mass spectra were acquired on a Finnigan MAT Model 8400 mass spectrometer. M-H-W Laboratories, Phoenix, AZ, performed elemental analyses.

X-ray Structure Determinations. The structure data for **4** have been deposited in conjunction with the preliminary communication (Cambridge Crystallographic Data Center No. CCDC-187182).[34] In addition, the crystallographic details of **8**, **13**, and **16** are gathered in the Supporting Information. All data were collected on a Bruker Apex CCD diffractometer at 100(2) K with Mo Kα radiation (λ = 0.710 73 Å).

Relevant data for the crystallographically studied compounds are summarized in Table 1.

Efficient Preparation of [1 Cp*-1-H-*arachno*-1-IrB_4H_9] (1). The original synthetic procedure afforded moderate net yields of [Cp*IrB_4H_{10}] (**1**), starting from [Cp*$IrCl_2$]$_2$ and monoborane reagents.[12] The main drawback of this preparation was the fact that the reaction of [Cp*$IrCl_2$]$_2$ with $LiBH_4$ gave a 1:1 mixture of [1-Cp*-1-(H)$_2$-*arachno*-1-IrB_3H_7] (**2**) and [Cp*IrH_4]. This iridium hydride was consequently separated to give pure iridatriborane **2**, which is the final precursor to **1**. In addition, we have found that the ratio of **2** and [Cp*IrH_4] depends on the warming rate of the reaction mixture from low temperatures to room temperature; thus, we have obtained **2**:[Cp*IrH_4] proportions of, for example, 1:7. However, we have recently demonstrated that some metal hydrides are good

(33) Shriver, D. F.; Drezdzon, M. A. *The Manipulation of Air-Sensitive Compounds*, 2nd ed.; Wiley-Interscience: New York, 1986.
(34) Macias, R.; Fehlner, T. P.; Beatty, A. M. *Angew. Chem., Int. Ed.* **2002**, *41*, 3860−3862.

precursors for the synthesis of metallaboranes.[16] Thus, we considered that the reaction of the byproduct, [Cp*IrH_4], with BH_3THF could also lead to the *arachno*-iridapentaborane **1**. This supposition was found to be true, and now we can prepare **1** in a high-yield one-pot reaction.

In a typical synthesis, 91 mg (0.12 mmol) of [Cp*$IrCl_2$]$_2$ in THF under argon at −40 °C was treated with 5-fold excess of $LiBH_4$ (2 M in THF). The resulting suspension was allowed to reach room temperature to give a yellow solution. At this point the reaction mixture contained mainly **2**, [Cp*IrH_4], and $LiBH_4$. To this mixture was added a 10-fold excess of BH_3·THF (1 M in THF), and the resulting yellow solution was heated at 60 °C for 2 days. The solvent was evaporated to dryness and the residue extracted with hexane and filtered through Celite to give a pale yellow solution. Crystallization from hexane gave 84 mg (0.22 mmol, 95%) of [Cp*IrB_4H_{10}] (**1**).

Reaction of [Cp*IrB_4H_{10}] (1) with PMe_3. A 15 mg portion (0.04 mmol) of **1** was dissolved in 0.7 mL of C_6D_6 and placed in a 5 mm NMR tube, together with a capillary containing an acetone-d_6 solution of [Et_4N][B_3H_8] as external reference. To this starting solution was added 0.09 mmol of PMe_3 (1 M solution in THF) under an argon atmosphere at room temperature. ^{11}B NMR of the reaction mixture showed the formation of two new species, plus BH_3·PMe_3. The major component of the mixture was characterized as [1-(Cp*)-1-(H)-*arachno*-1-IrB_3H_6-2-(PMe_3)] (**3**). The reaction mixture was transferred from the NMR tube to a Schlenk flask and evaporated to dryness under vacuum. This procedure removed the excess of PMe_3 and the borane adduct BH_3·PMe_3. The resulting yellow residue was subsequently kept in the refrigerator under argon for 2 days. After this time, compound **3** was converted quantitatively to the second metallaborane, a minor component in the first steps of the reaction. Crystallization from hexane at low temperatures gave 12 mg (0.03 mmol, 69% yield) of **4**.

[1-(Cp*)-1,1-$(H)_2$-*arachno*-1-IrB_2H_4-2-(PMe_3)] (4). IR (KBr): 2407 (s, ν_{B-H}), 2390 (s, ν_{B-H}), 2373 (s, ν_{B-H}), 2295 (m, ν_{B-H}), 2153 (s, ν_{Ir-H}). HRMS (EI): *m*/*z* 430 ($M^+ - H_2$); calcd for $C_{13}H_{28}B_2PIr$ 430.174 78 ($M^+ - H_2$), measd 430.173 17. Anal. Calcd for $C_{13}H_{30}B_2PIr$: C, 36.21; H, 7.01. Found: C, 36.40; H, 6.99.

[1-(Cp*)-1-(H)-*arachno*-1-IrB_3H_6-2-(PMe_3)] (3). ^{11}B NMR (C_6D_6): δ −5.3 (d, ^1J(BH) = 134; {^{1}H}, s, 1B), −12.9 (t, ^1J(BH) = 109, 1B), −20.1 (t, ^1J(BH) + ^1J(BP) = 112; {^{1}H}, d, ^1J(BP) = 103 Hz, 1B). ^{1}H{^{11}B} NMR (C_6D_6): δ 3.96 (br. s, 1H, BH_t), 3.07 (s, 1H, BH_t), 2.45 (dd, ^2J(HH) = 7, ^2J(HP) = 19, BH_t), 2.11 (s, 15 H, Cp*), 1.99 (s, 1H, B−H_t), 0.63 (d, ^2J(HP) = 11, 9H, Me), −4.32 (quint, ^2J(HH) = 6.9, 1H, BHB), −4.78 (dq, 1H, ^2J(HH) = 6.6, ^2J(HP) = 19.2, BHB), −18.50 (d, ^3J(HP) = 21, 1H, IrH). ^{31}P{^{1}H} NMR (C_6D_6): δ −9.7 (br q, ^1J(BP) = 10.0, PMe_3). IR (hexane): 2518 (w, ν_{B-H}), 2472 (m, ν_{B-H}), 2425 (s, ν_{B-H}); 2145 (s, ν_{Ir-H}). LR-MS(EI): *m*/*z* 444 (M^+); calcd for $C_{13}H_{31}B_3IrP$, found envelope with cutoff at 445 and maximum at 442; the isotopic pattern suggests that the ions M^+ and $M^+ - H_2$ are overlapped with a major contribution of the latter.

Reaction of [Cp*IrB_4H_{10}] (1) with PMe_2Ph. A 12 mg (0.03 mmol) portion of **1** was treated with a 10-fold excess of PMe_2Ph under the same conditions as for the PMe_3 reaction above. Integration versus the external reference showed quantitative reaction to give BH_3·PMe_2Ph and [1-(Cp*)-1-(H)-*arachno*-1-IrB_3H_6-2-(PMe_2Ph)] (**5**). The reaction mixture was evaporated to dryness under vacuum, giving a pale yellow precipitate that was kept under argon at low temperatures for 18 h. After this time, compound **5** converted to [1-(Cp*)-1,1-$(H)_2$-*arachno*-1-IrB_2H_4-2-(PMe_2Ph)] (**6**). At this point, the reaction gave mainly **6** and the borane adduct, which were separated by thin-layer chromatography (TLC) on silica gel in air, using CH_2Cl_2−hexane (1:5) as eluent. A colorless UV-active band (R_f = 0.3) was removed from the TLC plate, giving 1 mg (0.002 mmol, 7%) of **6** as a pale-yellow solid.

[Cp*IrB_2H_6(PMe_2Ph)] (6). IR (KBr): 2403 (s, ν_{B-H}), 2368 (s, ν_{B-H}), 2299 (m, ν_{B-H}), 2151 (s, ν_{Ir-H}). LRMS (EI): *m*/*z* 494 (M^+); calcd for $C_{18}H_{32}B_2PIr$, found envelope with cutoff at 495 and maximum at 490, which suggests that the ions M^+ and $M^+ - H_2$ are overlapped. Anal. Calcd: C, 43.83; H, 6.54. Found: C, 44.00; H, 6.70.

[1-(Cp*)-1-(H)-*arachno*-1-IrB_3H_6-2-(PMe_2Ph)] (5). ^{11}B NMR (C_6D_6): δ −5.7 (br d, ^1J(BH) = 106; {^{1}H}, s, 1B), −12.7 (t, ^1J(BH) = 101, 1B), −19.3 (t, ^1J(BH) + ^1J(BP) = 98; {^{1}H}, d, ^1J(BP) = 97, 1B). ^{1}H{^{11}B} NMR (C_6D_6): δ 7.48 (m, 1H, Ph), 7.30 (m, 2H, Ph), 7.02 (m, 2H, Ph), 3.98 (br. s, 1H, BH_t), 3.15 (s, 1H, BH_t), 2.85 (dd, ^2J(BP) = 17, ^1J(BH) = 7, 1 H, BH_t), 2.17 (s, 1H, BH_t), 2.08 (s, 15 H, Cp*), 1.09 (d, ^2J(HP) = 11.3, 3H, Me), 0.99 (d, ^2J(HP) = 11.3, 3H, Me), −4.24 (s, 1H, BHB), −4.44 (dq, ^2J(BP) = 18.9, ^2J(BH) = 6.5, 1H, BHB), −18.19 (d, ^3J(HP) = 21, 1H, IrH). ^{31}P{^{1}H} NMR (C_6D_6): δ -5.3 (v br q, ^1J(BP) = 14.0, PMe_2Ph). HRMS (EI): *m*/*z* 506 (M^+); calcd for $C_{18}H_{33}B_3IrP$ 506.2228 (M^+), measd 506.2223.

Reaction of [Cp*IrB_4H_{10}] (1) with $PMePh_2$. Following the same procedure as above, 0.047 mL (0.25 mmol) of PMe_2Ph was added to 18 mg (0.05 mmol) of **1**. A few minutes after addition of the phosphine, the ^{1}H and ^{11}B NMR spectra showed that the starting material reacted quantitatively to give BH_3·$PMePh_2$ and [1-(Cp*)-1-(H)-*arachno*-1-IrB_3H_6-2-($PMePh_2$)] (**7**). The reaction mixture was evaporated to dryness under vacuum and the residue kept under argon for 2 days. After this time, NMR data demonstrated that compound **7** was transformed into [1-(Cp*)-1,1-$(H)_2$-*arachno*-1-IrB_2H_4-2-($PMePh_2$)] (**8**). The reaction mixture at this point contained mainly compound **8** and BH_3·$PMePh_2$, which were separated by thin-layer chromatography (TLC) on silica gel in air, using CH_2Cl_2−hexane (1:1) as eluent. A colorless UV-active band was removed at the bottom of the plate, yielding 5 mg (0.007 mmol, 14%) of **8** as a pale yellow solid.

[Cp*IrB_2H_6($PMePh_2$)] (8). IR (hexane): 2445 (s, ν_{B-H}), 2389 (s, ν_{B-H}), 2305 (w, ν_{B-H}), 2135 (m, ν_{Ir-H}). HRMS (FAB): *m*/*z* 556 (M^+); calcd for $C_{23}H_{34}B_2IrP$ 556.2214, (M^+), measd 556.2187. Anal. Calcd: C, 49.74; H, 6.17. Found: C, 49.92; H, 6.26.

[1-(Cp*)-1-(H)-*arachno*-1-IrB_3H_7-2-($PMePh_2$)] (7). ^{11}B NMR (C_6D_6): δ −5.9 (br), −12.3 (br), −19.1 (br). ^{1}H{^{11}B} NMR (C_6D_6): δ 7.40−7.06 (m, 10 H, C_6H_5), 3.96 (br, 1H, BH), 3.20 (br, 1H, BH), 3.11 (br, 1H, BH), 2.19 (br, 1H, BH), 1.97 (s, 15H, Cp*), 1.44 (d, 3H, Me), −4.11 (br, 1H, BHB), −4.20 (br, 1H, BHB), −17.95 (d, ^3J(HP) = 21 Hz, 1H, IrH). ^{31}P NMR (C_6D_6): δ 1.1 (br). HRMS (EI): *m*/*z* 568 (M^+); calcd for $C_{23}H_{35}B_3IrP$ 568.2385 (M^+), measd 568.2377.

Reaction of [Cp*IrB_4H_{10}] with PPh_3. To a C_6D_6 solution of **1** (11 mg, 0.03 mmol), we added 38 mg (0.14 mmol) of PPh_3 in a NMR tube under an argon atmosphere. After addition of the phosphine, there was no reaction during the first few minutes. Four hours later, there were small amounts of **1**, but the NMR data showed the formation of new species, which were characterized as [1-Cp*-*nido*-1-IrB_4H_8] (**9**) and the iridatetraborane [1-Cp*-1-H-*arachno*-1-IrB_3H_6-2-(PPh_3)] (**10**). Both species underwent decomposition, giving rise to the formation of a mixture of [1-Cp*-1,1-$(H)_2$-*arachno*-1-IrB_2H_4-(PPh_3)] (**11**), BH_3·PPh_3, and an excess of PPh_3. TLC was performed on this mixture using hexane as eluent. PPh_3 was at the front of the chromatogram, but BH_3·PPh_3 and **11** were collected together almost at the bottom of the plate. NMR spectroscopy demonstrated significant decomposition of **11** after chromatography, and therefore, this compound could not be purified further.

[Cp*IrB_2H_6(PPh_3)] (11). HRMS (FAB): *m*/*z* 618 (M^+); calcd for $C_{28}H_{36}B_2IrP$ 615.2135 (M^+ − 3H), measd 615.2116.

[1-Cp*-*nido*-IrB_4H_8] (9). ^{11}B NMR (C_6D_6): δ −8.9 (dt, ^1J(BH) = 158, 34 Hz; {1H}, s, 4B). ^{1}H{^{11}B} NMR (C_6D_6): δ 2.08 (s, 15H, Cp*), 2.69 (t, ^2J(HH) = 7, 4H, BH_t), −4.09 (t, ^2J(HH) = 7, 4H, BHB). LRMS (EI): *m*/*z* 380 (M^+), calcd for $C_{10}H_{23}B_4Ir$; found envelope with cutoff at 380 and maximum at 376, which indicates overlap of ions, $M^+ - n(H_2)$ (n = 1, 2).

[1-Cp*-1-H-*arachno*-1-IrB$_3$H$_6$-2-(PPh$_3$)] (10). ^{11}B NMR (C_6D_6): δ −7.1 (br, 1B), −11.5 (br, 1B), −17.9 (br, 1B). ^{1}H{^{11}B} NMR (C_6D_6): δ 7.67 (m, C_6H_5), 6.99 (m, C_6H_5), 2.05 (s, 15H, Cp*), 3.80 (br. s, BH_t), 3.20 (br. s, BH_t), 3.09 (br. s, BH_t), 2.27 (br s, BH_t), −3.69 (d, ^2J(HP) = 21, 1H, BHB), −4.39 (br s, 1H, BHB), −17.39 (d, ^3J(HP) = 20, 1H, IrH). ^{31}P{^{1}H} NMR (C_6D_6): δ 4.8 (br, $BPPh_3$). LRMS (FAB): *m*/*z* 630 (M^+), calcd for $C_{28}H_{37}B_3IrP$; found envelope with cutoff at 631 and maximum at 628 ($M^+ - H_2$).

Reaction of [Cp*IrB$_4$H$_{10}$] (1) with Pyridine. To 32 mg (0.08 mmol) of **1** dissolved in C_6D_6 was added 0.03 mL (0.42 mmol) of pyridine. The pale yellow initial solution turned bright orange. A few minutes after the addition, ^{1}H and ^{11}B NMR spectra showed formation of new species together with the starting material, which was present in residual amounts 34 min after the first ^{11}B NMR spectrum. At this point, **9**, [1-Cp*-1-H-*arachno*-1-IrB$_3$H$_6$-2-(C_5NH_5)] (**12**), [1-Cp*-1,1-(H)$_2$-*arachno*-1-IrB$_2$H$_4$(C_5NH_5)] (**13**), and BH_3·(C_5NH_5) were the major species of the reaction mixture. Two days later, compounds **9** and **12** decomposed to give a mixture containing the borane adduct BH_3·(C_5NH_5) and the tiriridaborane **13**. The solvent was evaporated to dryness, and the yellow residue was dried for several hours under vacuum. The resulting yellow solid was extracted with hexane to give a bright yellow solution. Crystallization from hexane at low temperatures gave 29 mg (0.067 mmol, 79%) of **13**.

[Cp*IrB$_2$H$_6$(C$_5$NH$_5$)] (13). IR (KBr): 2411 (s, ν_{B-H}), 2395 (s, ν_{B-H}), 2309 (w, ν_{B-H}), 2178 (m), 2144 (m, ν_{Ir-H}). HRMS (FAB): *m*/*z* 435 (M^+); calcd for $C_{15}H_{26}B_2NIr$ 432.1646, [M^+ − 3H], measd 432.1650.

[Cp*IrB$_3$H$_7$(C$_5$NH$_5$)] (12). ^{11}B NMR (C_6D_6): δ 8.6 (d, ^1J(HB) = 128, 1B), −12.3 (br), −11.7 (accidental overlapping with BH_3·(C_5NH_5)), −13.9 (d, ^1J(HB) = 142, 1B). ^{1}H{^{11}B} NMR (C_6D_6): δ 8.15 (m, 2H, C_5NH_5), 6.40 (m, 1H, C_5NH_5), 6.02 (m, 2H, C_5NH_5), 5.02 (d, ^nJ(HH) = 7, 1H, BH_t), 4.20 (s, 1H, BH), 3.56 (s, 1H, BH_t), 2.17 (s, 15H, Cp*), 2.14 (s, 1H, BH_t), −1.54 (q, ^2J(H,H) = 7, 1H, BHB), −4.18 (quint, 1H, BHB), −18.24 (s, 1H, IrH). MS experiments were unsatisfactory, due probably to the instability of **12**.

Reaction of [Cp*IrB$_4$H$_{10}$] (1) with Et$_3$N. Under an argon atmosphere, 0.007 mL (0.052 mmol) of Et_3N was added to 10 mg (0.026 mmol) of **1**, dissolved in 0.7 mL of C_6D_6 in a 5 mm NMR tube. Six hours after addition of the amine, the ^{11}B and ^{1}H NMR spectra of the reaction mixture exhibited new peaks, but the major species was the starting iridapentaborane. Therefore, the resulting pale yellow solution was left overnight in the NMR tube at room temperature. The intensity of **1** decreased, and the new peaks were more intense. By comparison with the compounds above, the new species were identified as [Cp*IrB$_4$H$_8$] (**9**), [Cp*IrB$_3$H$_7$(NEt_3)] (**14**), and [Cp*IrB$_2$H$_6$(NEt_3)] (**15**), together with the borane adduct BH_3·NEt_3. Two days later, there was still some compound **1** in the reaction mixture; on the other hand, integration of the ^{11}B NMR spectrum versus the external reference (capillary containing a solution of [NMe_4][B_3H_8] in acetone-d_6) demonstrated that the concentration of compound **14** decreased and, in contrast, compound **15** increased in concentration. After 6 days, the initial **1** reacted fully and compounds **9** and **14** decomposed to give a mixture of **15** and borane adduct. The final total boron concentration of the reaction mixture was half of the initial concentration. The reaction mixture was transferred from the NMR tube to a Schlenk tube, the solvent evaporated, and the residue extracted with hexane. ^{11}B NMR spectroscopy on a sample of the hexane-soluble fraction exhibited very weak signals, indicating decomposition of the iridatriborane **15**.

[Cp*IrB$_3$H$_7$(NEt$_3$)] (14). ^{11}B NMR (C_6D_6): δ 10.9 (d, ^1J(B,H) = 122, 1B), −12.7 (accidental overlap with BH_3·NEt_3), −13.2 (accidental overlap with BH_3·NEt_3). ^{1}H{^{11}B} NMR (C_6D_6): δ 2.57 (q, ^2J(H,H) = 7 Hz, 3H, Et), 2.06 (s, 15H, Cp*), 3.95 (d, ^2J(H,H) = 7 Hz, 1H, BH_t), 3.25 (br s, 1H, BH_t), 3.49 (br s, 1H, BH_t), 1.12 (t, ^3J(H,H) = 7, 3H, Et), −2.93 (q, ^2J(H,H) = 7, 1H, BHB), −4.53 (br s, 1H, BHB), −18.99 (s, 1H, IrH). MS experiments were unsatisfactory, due probably to the instability of **14**.

[Cp*IrB$_2$H$_6$(NEt$_3$)] (15). ^{11}B NMR (C_6D_6): δ 2.3 (d, ^1J(B,H) = 122, 1B), −23.4 (br t, ^1J(B,H) = 123, 1B). ^{1}H{^{11}B} NMR (C_6D_6): δ 2,79 (br. s, 1H, BH_t), 1.99 (s, 15H, Cp*), 0.65 (t, ^3J(H,H) = 8, 3H, Et), −4.87 (q, ^2J(H,H) = 8, 1H, BHB), −17.46 (s, 1H, IrH), −19.23 (s, 1H, IrH). MS experiments were unsatisfactory, due probably to the instability of **15**.

Reaction of [Cp*IrB$_3$H$_9$] with PMe$_3$. A 33 mg portion (0.04 mmol) of [Cp*$IrCl_2$]$_2$ was treated in THF with a 5-fold excess of $LiBH_4$ at −40 °C, while allowing the reaction mixture to reach the room temperature slowly over a period of 2 h. The solvent was evaporated to dryness and the residue extracted with hexane to give a yellow solution. ^{11}B NMR spectroscopy showed that [Cp*IrB$_3$H$_9$] was the only boron-containing compound in the final reaction mixture; however, the ^{1}H NMR spectrum demonstrated the presence of [Cp*IrH$_4$] as the major component.

Monitoring the ^{11}B NMR spectrum of the above mixture versus the external reference, we added an excess of PMe_3, resulting in the quantitative formation of **4** in just a few minutes.

Reaction of [Cp*IrB$_3$H$_9$] (2) with PMe$_2$Ph. A 3 mg portion (0.01 mmol) of **2** was dissolved in C_6D_6 and placed in an NMR tube with an external reference. To this solution, we added 0.007 mL (0.05 mmol) of PMe_2Ph under argon. ^{11}B and ^{1}H NMR spectra of the reaction mixture a few minutes after the addition showed quantitative formation of **6**.

Reaction of [Cp*IrB$_3$H$_9$] (2) with PMePh$_2$. Under the same conditions as above, 3 mg (0.01 mmol) of **2** was treated with a 5-fold excess of $PMePh_2$ to give compound **8**. The reaction is quantitative by NMR.

Reaction of [Cp*IrB$_3$H$_9$] (2) with PPh$_3$. A 6 mg portion (0.016 mmol) of **2** was dissolved in C_6D_6 and treated with 21 mg (0.081 mmol) of PPh_3 at room temperature under argon. One hour after the addition of the phosphine, the concentration of **2** was half of its initial value; 4 h later, the reaction was complete with quantitative formation of **11**.

Reaction of [Cp*IrB$_3$H$_9$] (2) with py. An 8 mg portion (0.02 mmol) of **2** was treated with a 5-fold excess of pyridine (0.1 mmol) at room temperature under an argon atmosphere to give [Cp*IrB$_2$H$_6$(py)] (**13**). The reaction was quantitative by NMR and took place in a few minutes.

Reaction of [Cp*IrB$_3$H$_9$] (2) with NEt$_3$. An 8 mg portion (0.02 mmol) of **2** was treated with 0.02 mL (0.14 mmol) of NEt_3 in C_6D_6. The reaction was complete in about 16 h to give **15** quantitatively.

Reaction of [Cp*IrB$_2$H$_6$(PMe$_3$)] (3) with BH$_3$·THF. A 10 mg portion (0.023 mmol) of **3** was dissolved in 0.7 mL of C_6D_6 and the solution placed in a 5 mm NMR tube with an external reference (capillary containing a $(CD_3)_2CO$ solution of [Et_4N][B_3H_8]). This starting solution was monitored by ^{11}B NMR, and then 0.5 mL of BH_3·THF (1 M) was added under an atmosphere of nitrogen at room temperature. After a few minutes, the ^{11}B NMR spectrum of the reaction mixture showed quantitative conversion of **3** to give the starting iridaborane **1**.

Reaction of [Cp*IrB$_3$H$_7$(PMe$_3$)] (4) with BH$_3$·THF. A 15 mg portion (0.04 mmol) of **1** was treated with an excess of PMe_3 under the same conditions as above. At this point, the reaction mixture had compounds **4** and **3** in a 18:1 ratio. To this mixture was added an excess of BH_3·THF under a nitrogen atmosphere at room temperature to give a mixture of **1** and **2** in a 15:1 ratio. The total boron intensity before and after the addition of BH_3·THF versus the external reference is maintained, indicating a quantitative reversible reaction.

Reaction of [Cp*IrB$_3$H$_7$(PMe$_2$Ph)] (5) with BH$_3$·THF. Using the same conditions and procedure as for the PMe_3 derivatives above, 3 mg (0.01 mmol) of **1** was treated with a

5-fold excess of PMe_2Ph to give compound **5** quantitatively and also BH_3·PMe_2Ph. To this mixture was added an excess of BH_3·THF to afford the starting iridaborane **1.** The conversion is quantitative.

Reaction of [Cp*IrB$_2$H$_6$(PMe$_2$Ph)] (6) with BH$_3$·THF. The reaction mixture above was treated again with an excess of PMe_2Ph and then evaporated under vacuum, resulting in a yellow residue that was kept under an argon atmosphere at room temperature for 2 days. This residue was dissolved in C_6D_6 and examined by ^{11}B and ^1H NMR. The sample was, therefore, a combination of compound **6** and a large excess of BH_3·PMe_2Ph. To this mixture, we added an excess of BH_3·THF, leading to the formation of **2**. The integrals versus the external reference demonstrated quantitative conversion between the iridaboranes.

Reaction of [Cp*IrB$_3$H$_7$(PMePh$_2$)] (7) with BH$_3$·THF. Following the general procedures described above for the PMe_3 and PMe_2Ph derivatives, we added a 5-fold excess of $PMePh_2$ to a solution of **1** (4 mg, 0.01 mmol) in C_6D_6 to give **7** and BH_3·$PMePh_2$; then we added an excess of BH_3·THF to recover the starting iridaborane quantitatively.

Reaction of [Cp*IrB$_2$H$_6$(PMePh$_2$)] (8) with BH$_3$·THF. The reaction mixture above was treated with an excess of $PMePh_2$, evaporated under vacuum, and kept under argon for 2 days. This residue contained **8** and a large excess of BH_3·$PMePh_2$. We added an excess of BH_3THF, regenerating **2**. The boron intensities of the final iridaborane matched those of the starting phosphine derivative.

Reaction of [Cp*IrB$_2$H$_6$(py)] (13) with BH$_3$·THF. A sample of **13**, which was not weighed, was treated with an excess of BH_3·THF, yielding **2**. The concentration of the final iridatetraborane was the same as that of the initial pyridine derivative, demonstrated by integration versus the external reference.

Reaction of [Cp*IrB$_2$H$_6$(NEt$_3$)] (15) with BH$_3$·THF. We added an excess of BH_3·THF to a unweighed sample of **15**. The conversion to **2** was quantitative.

Reaction of [Cp*IrB$_4$H$_{10}$] (1) with Br$_2$. A 64 mg portion of **1** (0.17 mmol) was placed in a Schlenk tube under an argon atmosphere and then treated with 0.01 mL of Br_2 (0.34 mmol) at room temperature. Gas was released immediately, and the resulting orange solution was stirred at room temperature for 2 h. The solvent was evaporated to dryness under vacuum to give an orange residue, which was extracted with hexane to afford a yellow solution and an orange residue. The hexane fraction was concentrated under vacuum and placed in the freezer at −40 °C to give colorless crystals of the dibromo derivative [Cp*IrB$_4$H$_8$Br$_2$] (**16**; 42 mg, 0.08 mmol, 46%). IR (KBr): 2517 (s, $\nu_{B-H;}$ sh, at 2544 and 2496), 2185 (m, ν_{Ir-H}), 1008 (s; sh, at 1040), 955 (m, ν_{B-Br}), 867 (m, ν_{B-Br}). HRMS (FAB): *m*/*z* calcd for $C_{10}H_{22}B_4Br_2Ir$, 537.0090, $[M - 1]^+$; found, 537.0123. Anal. Calcd for $C_{10}H_{23}B_4Br_2Ir$: C, 22.30; H, 4.30. Found: C, 22.44; H, 4.35.

In the reaction mixture, we detected a second iridaborane as a minor component, which was characterized by NMR as the monobromo derivative **17**.

[Cp*IrB$_4$H$_9$Br] (17). $^{11}B\{^1H\}$ NMR (C_6D_6): δ −5.8 (s, 1B), −7.5 (s, 2B), −12.0 (br s, 1B). $^1H\{^{11}B\}$ NMR (C_6D_6): δ 4.16 (s, 1H, BH_t), 3.14 (s, 1H, BH_t), 2.76 (s, 1H, BH_t), 2.40 (s, 1H, BH_t), 1.58 (s, 15H, Cp*), −2.28 (s, 1H, BHB), −4.36 (s, 1H, BHB), −5.14 (br s, 1H, BHB), −13.34 (s, 1H, IrH).

Reaction of [Cp*IrB$_4$H$_{10}$] (1) with *N*-Bromosuccinimide. A 3 mL portion of CH_2Cl_2 was added under an argon atmosphere to a Schlenk tube containing 10 mg (0.03 mmol) of **1** and 8.4 mg (0.05 mmol) of *N*-bromosuccinimide. A yellow solution and a pale yellow precipitate were formed immediately. The reaction mixture was stirred for 2 h at room temperature, the solvent evaporated, and the orange residue extracted with hexane to give an orange insoluble residue and an orange solution. The hexane solution was concentrated under vacuum and placed at −40 °C to give 5 mg (0.009 mmol, 31%) of **16**.

NMR-Monitored Reactions. To investigate the relative reaction rate of **1** with different Lewis bases, to determine the reaction rate of the transformation of **3** to give the iridatriborane **4**, and to investigate possible mechanistic pathways, we carried out a series of experiments in which the reaction mixture was monitored periodically by NMR.

1. Relative Reaction Rate of [Cp*IrB$_4$H$_{10}$] (1) with PMe$_3$, py, and NEt$_3$. 1.1. Reaction of [Cp*IrB$_4$H$_{10}$] (1) with PMe$_3$ in a 5:1 Ratio. To 4 mg (0.01 mmol) of **1** dissolved in C_6D_6 in an NMR tube with the external reference as above, we added 0.05 mmol of PMe_3 under an argon atmosphere to give **3**. The reaction is quantitatively complete a few minutes after the addition of the phosphine.

1.2. Reaction of [Cp*IrB$_4$H$_{10}$] (1) with py in a 5:1 Ratio. A 6 mg portion (0.016 mmol) of **1** was treated with 0.08 mL (6 mg, 0.078 mmol) of pyridine in C_6D_6. Fourteen minutes after the addition of the base, the concentration of the starting iridapentaborane was half of the initial value; 20 min later, the concentration of **1** was residual, giving a mixture of **12** and **13**.

1.3. Reaction of [Cp*IrB$_4$H$_{10}$] (1) with NEt$_3$ in a 5:1 Ratio. We added 0.05 mL (0.05 mmol) of NEt_3 to 4 mg (0.01 mmol) of [Cp*IrB$_4$H$_{10}$] dissolved in C_6D_6. Six hours after the addition of the base, the concentration of the iridapentaborane was seven-ninths of its initial value; 2 days after the treatment, the concentration was one-third of the starting concentration, and after 5 days **1** reacted completely, affording **15**.

2. Reaction of [Cp*IrB$_4$H$_{10}$] (1) with PMe$_3$ in a 1:2 Ratio and the Conversion of 3 to 4. A 7 mg portion (0.018 mmol) of **1** was treated with 0.036 mmol of PMe_3 (1 M in THF) in a 5 mm NMR tube with an external reference at room temperature. The formation of **3** took place a few minutes after addition of the phosphine; 8 h later, the concentration of the iridatetraborane decreased by half, and 46 h after the initiation of the reaction, the conversion of to give the iridatriborane was complete. The decrease in the total boron intensity corresponded to the loss of a {BH} unit. A white solid was formed on the walls of the NMR tube. This product was insoluble in C_6D_6 and $CDCl_3$, but it was soluble in acetone-d_6. The ^{11}B NMR spectrum of this product exhibited a singlet, indicating that it is not a borane. In addition, the intensity of this peak versus the external reference was smaller than the total boron loss of the reaction: i.e., it did not account for the {BH} loss. First-order kinetic treatment gave a $t_{1/2}$ value of 6 h for the transformation of **3** into **4** at room temperature.

3. Reaction of [Cp*IrB$_4$H$_{10}$] (1) with PMe$_3$ in a 1:7 Ratio and the Conversion of 3 to 4. A 12 mg portion (0.03 mmol) of **1** was treated with 0.2 mL (0.2 mmol) of PMe_3 in C_6D_6 at room temperature. In contrast with the reaction above, 40 days after the addition of phosphine **3** was still present in the reaction mixture. The decrease of the concentration of **3** was parallel to the increase of **4**, [Cp*IrH$_4$], and the borane adduct BH_3·PMe_3.

4. Time-Dependent Behavior of the system [Cp*IrB$_4$H$_{10}$] (1) with PPh$_3$. We followed the reaction between **1** and PPh_3 at room temperature. This allowed the time-dependent behavior of the system to be investigated and, through this, the spectroscopic identification of **9** as an intermediate in the reaction pathway.

4.1. Reaction of [Cp*IrB$_4$H$_{10}$] (1) with PPh$_3$ in a 1:5 Ratio. To 11 mg (0.03 mmol) of **1** dissolved in 1 mL of C_6D_6, we added 38 mg (0.14 mmol) of PPh_3 under an argon atmosphere at room temperature. The reaction was monitored by ^1H and ^{11}B NMR spectroscopy at different intervals of time.

4.2. Reaction of [Cp*IrB$_4$H$_{10}$] (1) with PPh$_3$ in a 1:2 Ratio. A 5 mg portion (0.013 mmol) of **1** was treated with 6.9

mg (0.026 mmol) of PPh_3 in C_6D_6 at room temperature. The reaction was then studied by NMR.

5. Ligand Exchange Reactions. 5.1. Reaction of Compound 3 with PMe_2Ph. A 6 mg portion (0.016 mmol) of **1** was treated with 2 equiv of PMe_3 in toluene-d_8. To this reaction mixture was added a 20-fold excess of PMe_2Ph, and the reaction exchange was followed by NMR at low temperatures.

5.2. Reaction of Compound 4 with Lewis Bases. A 4 mg portion (0.009 mmol) of compound **4** was treated in toluene-d_8 with a 20-fold excess of PMe_2Ph, $PMePh_2$, PPh_3, and py, respectively. The respective reaction mixtures were studied by NMR at different temperatures.

Acknowledgment. This work was supported by the National Science Foundation (Grant Nos. CHE 9986880 and CHE 0304008).

Supporting Information Available: Tables and figures giving NMR integrals for the monitoring of the reactions and the exchange experiments and tables giving X-ray diffraction details, atomic coordinates, bond lengths and angles, and isotropic and anisotropic displacement parameters; crystal data are also available as CIF files. This material is available free of charge via the Internet at http://pubs.acs.org.

OM049960A